

# Femtosecond Bessel-beam-assisted high-aspect-ratio microgroove fabrication in fused silica

Liangliang Zhao (赵亮亮)<sup>1</sup>, Feng Wang (王锋)<sup>1</sup>, Lan Jiang (姜澜)<sup>1</sup>, Yongfeng Lu (陆永枫)<sup>2</sup>, Weiwei Zhao (赵巍巍)<sup>1</sup>, Jun Xie (谢俊)<sup>1</sup>, and Xiaowei Li (李晓炜)<sup>1,\*</sup>

<sup>1</sup>Laser Micro/Nano-Fabrication Laboratory, School of Mechanical Engineering, Beijing Institute of Technology, Beijing 100081, China

<sup>2</sup>Department of Electrical Engineering, University of Nebraska-Lincoln, Lincoln, Nebraska 68588-0511, USA

\*Corresponding author: lixiaowei@bit.edu.cn

Received December 10, 2014; accepted February 12, 2015; posted online March 18, 2015

A simple and repeatable method to fabricate high-aspect-ratio (HAR) and high-quality microgrooves in silica is reported. The method consists of two steps: (1) formation of laser-modified regions by femtosecond Bessel beam irradiation, and (2) removing laser-modified regions through HF etching. Uniform, straight microgrooves can be fabricated and the highest aspect ratio that can be reached is  $\sim 52$ . The phenomenon is attributed to the uniform energy distribution in the long propagation distance, which leads to the long and uniform laser-modified regions and subsequent HF acid etching of laser-modified regions with high selectivity. This method will have potential applications in fabrication of HAR microgrooves in transparent materials.

OCIS codes: 140.3390, 230.4000, 320.5540.

doi: 10.3788/COL201513.041405.

Transparent, wide-band-gap materials have extensive applications in microfluids, microsensors, and other fields. Among these materials, fused silica has been widely used in the microfluidic systems due to its unique advantages, such as very high chemical stability, good electrical insulation properties, and wide optical transmission bandwidth<sup>[1]</sup>. High-aspect-ratio (HAR) microstructures are the core components of the previously mentioned applications<sup>[2-4]</sup>. Femtosecond lasers are very promising for the fabrication of transparent dielectrics for photonic and optoelectronic devices due to its ultra-short pulse duration, ultra-high power densities, three-dimensional (3D) ultra-precision, and other unique advantages<sup>[5,6]</sup>.

Many studies have been conducted on the fabrication of HAR micro-channels by femtosecond lasers<sup>[7-11]</sup>. Marcinkevičius *et al.* fabricated 3D microchannels using femtosecond laser irradiation and chemical etching<sup>[8]</sup>. Bhuyan *et al.* applied femtosecond Bessel beams to fabricate taper-free microchannels and effectively improved the aspect ratio<sup>[10]</sup>. Jiang *et al.* reported a method called polarization-independent etching of fused silica by shaped femtosecond pulse trains to fabricate HAR microchannels<sup>[11]</sup>. The previous reports have proved the feasibility of femtosecond laser fabrication of HAR micro-channels in fused silica, but the fabrication of HAR microgrooves, which are often used to make piezoelectric microgyroscopes, microbalancers, microresonators, and optical transmission elements<sup>[12-15]</sup>, has been little focused on.

In this Letter, we propose an effective method of femtosecond Bessel beam irradiation followed by chemical etching (FBLICE) to fabricate HAR microgrooves with small width of  $\sim 10 \mu\text{m}$  in silica glass. Bessel beams maintain near-constant profile over distances far larger than the Rayleigh length of Gaussian beams, allowing for uniform

energy distribution in the long propagation distance<sup>[16-18]</sup>. Therefore, the first step is to produce deep laser-modified regions with relatively very small width by femtosecond Bessel beam irradiation. Then the HAR microgrooves are finally formed after laser-modified regions being etched with HF acid solution in high selectivity. The results indicate that by converting laser energy distribution profile of Gaussian to Bessel and combination with HF acid etching, straight and smooth microgrooves with aspect ratio of  $\sim 52$  can be fabricated. This method will have potential applications in the fabrication of multilayer microfluidic devices, microsensors, and other devices in microelectromechanical systems (MEMSs).

The schematic diagram of the experimental setup is showed in Fig. 1. A 3.5 W amplified Ti: sapphire femtosecond laser system (Spectra Physics Spitfire) is used to generate femtosecond laser pulses (800 nm, 50 fs, 1 kHz, Gaussian type). A half-wave plate and a polarizer are combined to adjust the pulse energy continuously.

As the most cost-effective and convenient way to generate a Bessel beam<sup>[19]</sup>, an axicon (base angle  $\alpha$  is  $2^\circ$ , beam width is 6 mm) is used. As shown in Fig. 1, the initial Bessel beam is created right after the action, while in the far-field a ring-shaped profile is produced. Furthermore, in order to reduce the Bessel beam size and increase the laser fluence, a plano-convex lens (focal length  $f_1 = 150 \text{ mm}$ ) compromised with a  $10\times$  microobjective (NA = 0.30, focal length  $f_2 = 16 \text{ mm}$ ) are used to demagnify the initial Bessel beams to a microscale by a parameter of  $f_1/f_2 = 9.375$  and the distance between the two objectives is adjusted to be the sum of  $f_1$  and  $f_2$ . The fused silica with a thickness of  $1000 \mu\text{m}$  is fixed on a computer-controlled six-dimensional translation stage (PIM-840.5DG) with translation precision of  $1 \mu\text{m}$  in the  $x$ - and  $y$ -directions

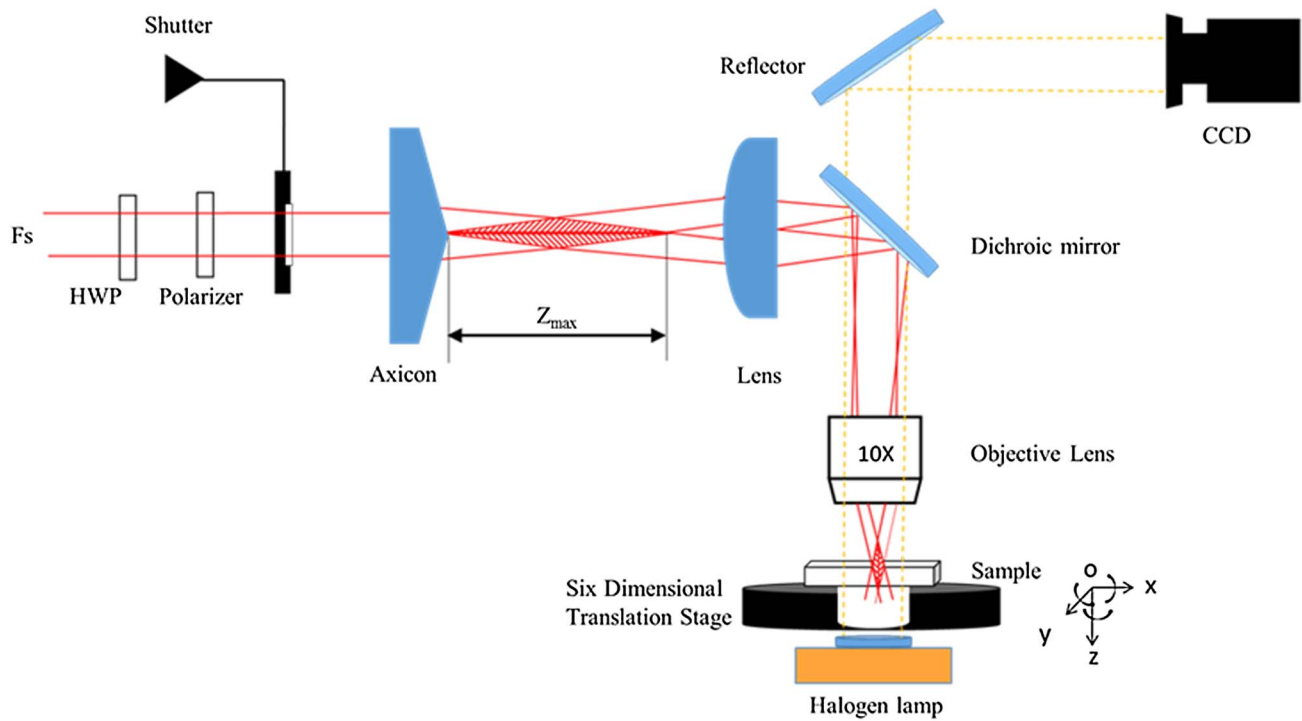


Fig. 1. Schematic diagram of the femtosecond Bessel beams irradiation. Beam propagation direction is along  $z$ -axis. HWP, half-wave plate;  $Z_{\max}$ , focal depth of the initial Bessel beams.

and  $0.5 \mu\text{m}$  in the  $z$ -direction. The demagnified Bessel beams are projected in the sample from its top surface. All of the pulse energies mentioned in our work are measured right before the  $10\times$  objective lens.

The scanning direction is set along the  $y$ -axis, which is the polarization direction of the incident laser. The scanning length is  $500 \mu\text{m}$  for each scanning line and the distance between each two lines is adjusted at  $100 \mu\text{m}$  along the  $x$ -axis. A charge-coupled device (CCD) camera is used to observe the fabrication processes on the microscope system.

To characterize the morphology of laser-modified regions, the cross section of the sample is observed by optical microscope after femtosecond Bessel beam irradiation. Then the sample with laser-modified regions is put into HF solution with concentration of 10% in ultrasonic cleaner for 2 h. The fused silica should be polished with waterproof abrasive papers along the cross section ( $xoz$ -plane), which is perpendicular to  $y$ -axis, to a random position after etching in order to observe the microgrooves induced inside silica. Then the polished fused silica is cleaned with distilled water and alcohol in ultrasonic cleaner for about 10 min, respectively. Ultimately, scanning electron microscopy (SEM) and optical microscope are used to characterize the cross section of microgrooves.

Figure 2 illustrates the cross sectional optical image of the laser-modified regions in fused silica. The pulse energy is  $40 \mu\text{J}$  and the scanning speed is  $5 \mu\text{m/s}$ . Shallow grooves are already formed in the front surface ( $xy$ -plane), while laser-modified regions are formed at the other irradiated zones along the longitudinal direction of the femtosecond

laser transmission, after the femtosecond Bessel beam irradiation. In the scanning process, laser-modified regions created on one side, with different refractive index from untreated glass, changed the propagation path of some rays. But this does not influence the stability of Bessel beams. Bessel beams are constructed as a superposition of plane waves propagating on a cone. In this case, although the small laser modified regions affects the interference of a few rays, other plenty of rays will interfere and form the Bessel beams.

As shown in Fig. 2, the straight and uniform laser modified regions are clearly visible. The depth of the laser modified regions can reach  $1000 \mu\text{m}$  (equal to the thickness of the material), while the width is only  $4 \mu\text{m}$  and the aspect ratio is  $\sim 250:1$ . The unique properties of Bessel beams, such as the extended depth and uniform energy distribution in the laser propagation direction<sup>[20,21]</sup>, are considered as a key factor to form such small, long, and uniform

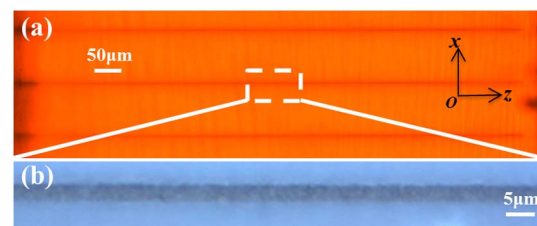


Fig. 2. (a) Cross-sectional optical image of laser-modified regions formed in fused silica by femtosecond Bessel beams irradiation at  $E = 40 \mu\text{J}$ ,  $v = 5 \mu\text{m/s}$  with their magnifications; (b) Beam propagation direction is along  $z$ -axis.

laser-modified regions. It is also important to note the laser power in unit volume is too small to remove the material due to the energy distribution in the extended propagation length.

In addition, three distinct types of femtosecond Bessel beams induced modifications in fused silica are identified: Type I modification with a smooth refractive index change, Type II modification with self-organized periodic nanogratings, and Type III modification with void-like domains<sup>[22,23]</sup>. The Type II and III regions are selective to chemical etching which can be distinguished with the region of Type I for its similar etching rate to the untreated glass. In the existing conditions, there is a characteristic opaque or dark region in bright-field due to the formation of scattered centers in fused silica (the Type III modifications), as shown in Fig. 2. The Type III modification is attributed to a high-pressure wave accompanied by the microexplosion. The decrease of the bridging angles of the  $\text{SiO}_4$  tetrahedrons in densified silica increases the reactivity of oxygen to HF acid<sup>[8]</sup>. Thus the etching rate of Type III modifications will be higher with respect to the etching rate of undamaged silica.

Figure 3(a) illustrates the cross sectional SEM images of the microgrooves. To investigate the repeatability of the geometry of the grooves, five microgrooves are produced in different locations at a certain interval of  $100\ \mu\text{m}$  along the  $x$ -axis for the same experimental condition ( $40\ \mu\text{J}$  pulse energy,  $5\ \mu\text{m/s}$  scanning speed, 10% HF acid solution, 2 h with ultrasonic cleaner assisting). The microgrooves extend into  $519.2\ \mu\text{m}$  in the interior of silica with the average width of  $\sim 10\ \mu\text{m}$ , that is to say the aspect ratio is  $\sim 52$ . The formation of the microgrooves is attributed to the chemical reaction of HF acid solution with laser-modified regions in high selectivity<sup>[24]</sup>.

The cross sectional morphologies of the grooves are slightly V-shaped (the angle between the two walls is less than  $5^\circ$ ) and the width at the entrance tends to be larger than at the buried end. This is due to the fact that the entrance of the grooves is exposed to the acid for a longer period of time because HF acid also etches pristine silica,

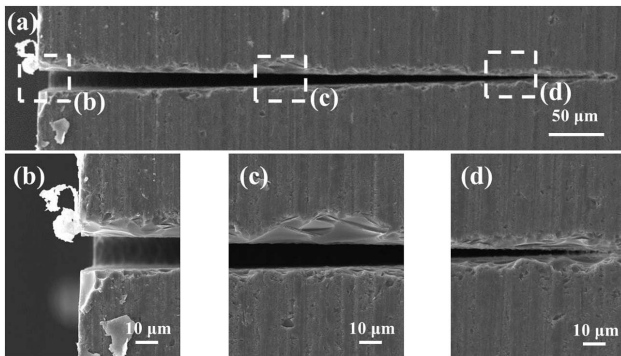


Fig. 3. (a) Cross sectional SEM images of the microgroove after HF etching at HF solutions with concentration of 10% in ultrasonic cleaner for 2 h; (b) magnification of the entrance of the groove; (c) magnification of the medium part of the groove; (d) magnification of the bottom part of the groove.

although at a slower rate than the irradiated regions. According to the cross sectional SEM image of the microgroove after HF etching, one can easily observe that the sidewall of the microgroove is very smooth with few microglass fragments left on. In addition, Figs. 3(b)–3(d) illustrates the magnifications of the entrance, medium, and bottom part of the microgrooves, respectively. It is worth noting the edge of the groove is a little destroyed and we attribute it to the destruction in the process of polishing with waterproof abrasive papers, but this does not influence the high quality of the microgrooves.

To research the dependence of aspect ratio of the microgrooves on the pulse energy, the different pulse energies of 10, 15, 20, 25, 30, 35, and  $40\ \mu\text{J}$  are used to fabricate the microgrooves, with the scanning velocity of  $5\ \mu\text{m/s}$ . It can be seen from the curve in Fig. 4 that an increase of incident pulse energy leads to an increase of the aspect ratio. When the incident pulse energy increases, the energy density at the tailing portion of Bessel beams will increase and reach a level where Type III laser modifications occur. Furthermore, this effect increases the laser-modified depth of Type III regions, while the width of laser-modified regions remains slightly increased with the increased pulse energy. The slight increase of the width combined with the relatively rapid increase of the depth cause an increase of the aspect ratio in laser-modified regions of Type III. The increase of pulse energy leads to more reduction of the bridging angles of the  $\text{SiO}_4$  tetrahedrons, which causes a more oxygen reactivity to HF acid. Thus, the higher pulse energy leads to a higher etch rate and this again facilitates a larger aspect ratio for a given etch time.

Although HAR microgrooves in fused silica have been fabricated, follow-up works are expected to further improve the aspect ratio and quality, and reduce the width of the microgrooves. First, the etching parameters, such as the concentration of HF acid and etch time, can be promising to achieve the objective. Furthermore, the chemical etching has the drawback of wasted time and inevitably

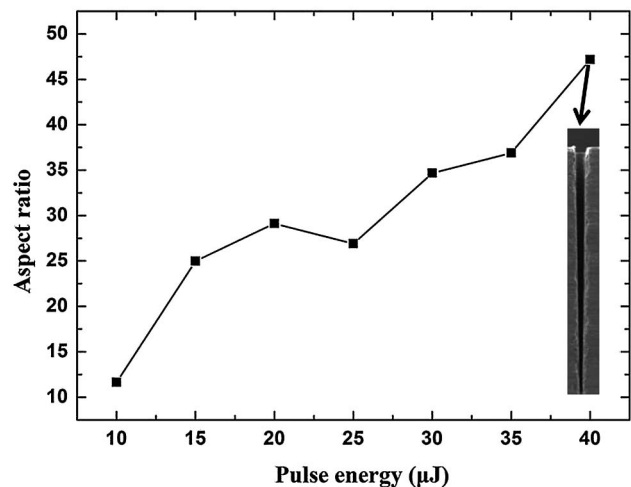


Fig. 4. Dependence curve of aspect ratio on the pulse energy and the scanning velocity is  $5\ \mu\text{m/s}$ , when the femtosecond Bessel beams were focused on the surface of the silica.

enlarges the width of the femtosecond Bessel-beam-modified regions. In order to solve the problems, the propagation length of Bessel beams can be appropriately adjusted to increase laser power in unit volume to directly remove the material without chemical etching.

In conclusion, fused silica microgrooves with aspect ratio of  $\sim 52$  are fabricated using femtosecond Bessel beams and chemical selectivity etching. First, laser-modified regions of great depth up to 1000  $\mu\text{m}$  with the width of  $\sim 4 \mu\text{m}$  are formed by femtosecond laser with laser energy distribution profile of Bessel beams. Then, HF solution is employed to remove the laser-modified regions and the smooth HAR microgrooves are formed. The formation of HAR grooves can be attributed to two aspects: (1) uniform energy distribution in the long propagation distance of femtosecond Bessel beams leads to long and uniform laser-modified regions, and (2) HF acid etching has a high selectivity of the Type II laser-modified regions. Furthermore, the aspect ratio of the microgrooves increases with the increase of the pulse energy. In addition, the etch factors in the case of fused silica are worthy of researching in follow-up work.

This work was supported by the National 973 Program of China (No. 2011CB013000) and the National Natural Science Foundation of China (Nos. 91323301 and 51305030).

## References

1. R. Osellame, H. Hoekstra, G. Cerullo, and M. Pollnau, *Laser Photon. Rev.* **5**, 442 (2011).
2. S. Ansari, Z. Ansari, H. Seo, G. Kim, Y. Kim, G. Khang, and H. Shin, *Sensors Actuat. B Chem.* **132**, 265 (2008).
3. K. Jensen, *MRS Bull.* **31**, 101 (2006).
4. W. Ong, J. Kee, A. Ajay, N. Ranganathan, K. Tang, and L. Yobas, *Appl. Phys. Lett.* **89**, 093902 (2006).
5. X. Long, J. Bai, X. Liu, W. Zhao, and G. Cheng, *Chin. Opt. Lett.* **11**, 102301 (2013).
6. Y. Ju, C. Liu, Y. Liao, Y. Liu, L. Zhang, Y. Shen, D. Chen, and Y. Cheng, *Chin. Opt. Lett.* **11**, 072201 (2013).
7. L. Jiang, P. Liu, X. Yan, N. Leng, C. Xu, H. Xiao, and Y. Lu, *Opt. Lett.* **37**, 2781 (2012).
8. A. Marcinkevičius, S. Juodkazis, M. Watanabe, M. Miwa, S. Matsuo, H. Misawa, and J. Nishii, *Opt. Lett.* **26**, 277 (2001).
9. Y. Li, S. Qu, and Z. Guo, *J. Micromech. Microeng.* **21**, 075008 (2011).
10. M. Bhuyan, F. Courvoisier, P. Lacourt, M. Jacquot, L. Furfaro, M. Withford, and J. Dudley, *Opt. Express* **18**, 566 (2010).
11. X. Yan, L. Jiang, X. Li, K. Zhang, B. Xia, P. Liu, L. Qu, and Y. Lu, *Opt. Lett.* **39**, 5240 (2014).
12. S. Lee, *J. Appl. Phys.* **40**, 5164 (2001).
13. L. Li, T. Abe, and M. Esashi, *Sensors Actuat. A Phys.* **114**, 496 (2004).
14. H. Jung, Y. Hwang, I. Hyeon, Y. Kim, and C. Baek, in *Proceedings of the 3rd IEEE Int. Conf. on Nano/Micro Engineered and Molecular Systems* 1172 (2008).
15. J. Jia, C. Zhou, and X. Sun, *Appl. Opt.* **43**, 2112 (2004).
16. M. Bhuyan, F. Courvoisier, and P. Lacourt, *Appl. Phys. Lett.* **97**, 081102 (2010).
17. M. Bhuyan, F. Courvoisier, and H. Phing, *Eur. Phys. J. Sp. Top.* **199**, 101 (2011).
18. J. Durnin, J. Miceli, and J. Eberly, *Phys. Rev. Lett.* **58**, 1499 (1987).
19. F. Courvoisier, P. Lacourt, M. Jacquot, and M. Bhuyan, *Opt. Lett.* **34**, 3163 (2009).
20. D. McGloin and K. Dholakia, *Contemp. Phys.* **46**, 15 (2005).
21. M. Duocastella and C. Arnold, *Laser Photon. Rev.* **6**, 607 (2012).
22. M. Bhuyan, P. Velpula, J. Colombier, T. Olivier, N. Faure, and R. Stoian, *Appl. Phys. Lett.* **104**, 021107 (2014).
23. M. Mikutis, T. Kudrius, G. Slekyš, D. Paipulas, and S. Juodkazis, *Opt. Mater. Express* **3**, 1862 (2013).
24. Y. Bellouard, A. Said, M. Dugan, and P. Bado, *Opt. Express* **12**, 2120 (2004).